Thin Solid Films 568 (2014) 31–37

Contents lists available at ScienceDirect

Thin Solid Films

journal homepage: www.elsevier.com/locate/tsf

Compositional tuning of yttrium iron garnet film properties by multi-beam pulsed laser deposition

Alberto Sposito [a,*], Gavin B.G. Stenning [b], Simon A. Gregory [b], Peter A.J. de Groot [b], Robert W. Eason [a]

[a] Optoelectronics Research Centre, University of Southampton, Southampton SO171BJ, United Kingdom
[b] Physics and Astronomy, University of Southampton, Southampton SO171BJ, United Kingdom

ARTICLE INFO

Article history:
Received 28 January 2014
Received in revised form 2 August 2014
Accepted 4 August 2014
Available online 9 August 2014

Keywords:
Pulsed laser deposition
Magnetic properties
Magneto-optical properties
Yttrium iron garnet
X-ray diffraction

ABSTRACT

We report an investigation of the effects of variation of composition on the properties of yttrium iron garnet films grown on yttrium aluminium garnet substrates by multi-beam pulsed laser deposition. The ferromagnetic resonance linewidth is used as a quality factor: a significant variation is noticed from changing composition, with an experimentally observed optimum at $Y_{3.5}Fe_{4.5}O_{12}$.

1. Introduction

Yttrium iron garnet ($Y_3Fe_5O_{12}$), often abbreviated as YIG, is a cubic crystal featuring ferromagnetic and magneto-optic properties, which can be used in different application fields, ranging from optical communications, where Faraday and Kerr effects in YIG can be exploited for optical isolators and rotators [1], to microwave, where phase shifters, circulators and filters can be made thanks to the magnetic properties and the narrow ferromagnetic resonance (FMR) linewidth of YIG at GHz frequencies [2].

YIG and magneto-optic garnet films can be grown by several deposition techniques, such as liquid phase epitaxy (LPE) [3], sputtering [4] and pulsed laser deposition (PLD). Although LPE allows the growth of very high-quality YIG layers, PLD has proven to be a relatively cheap, fast and versatile deposition method for several crystals, including garnets [5]; moreover it is possible to grow thermodynamically unstable materials, such as Bi:YIG and BIG (Bismuth Iron Garnet, $Bi_3Fe_5O_{12}$), which cannot be grown by LPE [6].

PLD-grown YIG films on GGG (Gadolinium Gallium Garnet, $Gd_3Ga_5O_{12}$) substrates with an FMR linewidth comparable to that of LPE-deposited YIG films on GGG [7] have recently been reported in [8]. More recently we have reported optimised PLD of YIG on YAG ($Y_3Al_5O_{12}$) substrates, which are cheaper than GGG and seem to induce better magnetic properties in the overgrown YIG layers [9]. However, single-beam PLD from a stoichiometric target usually leads to films that are iron (Fe) deficient, as previously reported in the literature [8] and confirmed in our experiments [9]. For this reason we have studied the composition and the effects of stoichiometric variation on the resultant properties of PLD-grown YIG films, whose yttrium (Y) and Fe concentration is varied by co-ablation of two separate targets of polycrystalline YIG with either an yttria (Y_2O_3) or an iron oxide (Fe_2O_3) target.

2. Experimental techniques

2.1. Fabrication

All YIG films were grown on 10×10 mm^2 $\times$ 1 mm-thick (100)-oriented YAG substrates in our multi-beam, multi-target ('multi-PLD' from now on) deposition chamber, described in detail in [10]. Up to three targets can be ablated with a KrF excimer laser, a Coherent COMPexPro 102F operating at $\lambda = 248$ nm (20 ns pulse duration), and two frequency-quadrupled Nd:YAG lasers, Continuum Surelite II-10 operating at $\lambda = 266$ nm (~5 ns pulse duration) with a fixed pulse repetition rate of 10 Hz. A Synrad J48-2W carbon dioxide (CO_2) laser operating at 10.6 μm (max. output power: 40 W) was used to heat the substrate during the deposition: the laser beam was raster-scanned on the back-side of the substrate, as described in [10]. The substrates were continuously rotated during the depositions to improve thickness uniformity. The targets were rotated and tilted continuously, in order to improve film homogeneity and ensure a uniform usage of the target surface. The targets used were a polycrystalline YIG target and sintered Y_2O_3 and Fe_2O_3 targets. The vacuum chamber was pumped down to a base

* Corresponding author.
E-mail address: as11g10@orc.soton.ac.uk (A. Sposito).

http://dx.doi.org/10.1016/j.tsf.2014.08.001
0040-6090/

Table 1
Summary table of targets and lasers used, as described in each section of this paper.

Section\targets	YIG	Fe_2O_3	Y_2O_3
3.1.1	KrF	–	–
3.1.2	Nd:YAG	–	–
3.2.1	Nd:YAG	KrF	–
3.2.2	KrF	Nd:YAG	–
3.3	Nd:YAG	–	KrF

pressure at least two orders of magnitude lower than the deposition value (i.e. $P_{base} < 0.068$ Pa), then filled with O_2.

The substrate temperature was set to the maximum value possible with this system, i.e. $T \approx 1150$ K, which is ~100 K lower than the optimum value we found for YIG growth on YAG (~1250 K) in our single-beam single-target PLD system. The duration of each deposition was set at ~72,000 laser pulses, unless otherwise stated.

Before starting the multi-PLD experiments, preliminary YIG depositions were performed in the multi-PLD chamber, in order to fine-tune the growth conditions of pure YIG and compare ablation of the YIG target with the KrF laser and the frequency-quadrupled Nd:YAG laser, as described in Section 3.1. Multi-PLD experiments of YIG and Fe_2O_3, performed to study the effect of Fe-deficiency compensation, are described in Section 3.2, and the results of multi-PLD of YIG and Y_2O_3 are discussed in Section 3.3. An important experimental point to note is that the Y_2O_3 target cannot be ablated with the Nd:YAG laser and for this reason the experiments with it were performed only with the laser set-up described below in Table 1.

2.2. Characterisation

The thickness of the YIG films was measured by a stylus profiler (KLA-Tencor P-16). Surface morphology was determined by optical microscopy and scanning electron microscope (Zeiss Evo 50), normally operated in variable pressure mode, with a 100 μm aperture, a voltage of 20 kV and a probe current of 2 nA. The composition was checked by energy-dispersive X-ray spectroscopy or EDX (Oxford Instruments INCA PentaFETx3), with a cobalt stub used for energy calibration before measurements and the stoichiometric YIG target and blank YAG substrates used for reference; oxygen concentration was assumed constant at 12 formula units (i.e. 60 at.%) and the accuracy of the concentration of the other elements was estimated as ~0.04 formula units. Crystallographic analysis was performed by X-ray diffraction or XRD (Bruker D2 Phaser, with a θ–θ configuration and a copper (Cu) X-ray source emitting at $K_{\alpha 1}$ and $K_{\alpha 2}$ wavelengths), with a resolution $\Delta 2\theta = 0.01°$. Transmission spectra were taken with the Varian Cary 500 Scan spectrophotometer. The broadband FMR spectroscopy was performed as described in [9,11], using a vector network analyser (HP E5071C) FMR technique (VNA-FMR), which allows FMR in the frequency range of 300 kHz to 20 GHz: the FMR linewidth of YIG films was measured with an accuracy of the order of 0.1 mT. The measurements were performed at a fixed excitation frequency of 6 GHz to ensure saturation of the sample within the applied field range available. DC magnetic fields of up to 0.6 T were available. For the characterisation of each film the applied magnetic field is swept while monitoring the scattering matrix parameter S_{21} (microwave absorption). This method reveals sub-mT features or 'satellites' of the main FMR mode. These modes can have several origins, such as (*i*) an increase in the intrinsic linewidth of the film by a process known as inhomogeneous broadening, as VNA-FMR excites only a very narrow frequency in time, and (*ii*) spin-waves and unresolved magnetostatic (dipolar) modes [12,13]. These arise from the geometry of the H_{RF} (microwave excitation field) with respect to the applied magnetic field H [14]. Both of these would contribute to obscuring the true intrinsic linewidth measurement for the film.

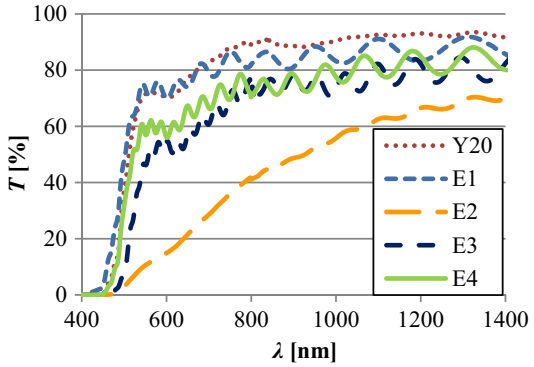

Fig. 1. Optical transmission spectra of E1–4 and Y20. Ripples are etalon fringes [15].

3. Results and discussion

3.1. Comparison of YIG ablation with different lasers

In this section we compare the ablation of a polycrystalline YIG target with two different lasers: a KrF excimer laser ($\lambda = 248$ nm) and a frequency-quadrupled Nd:YAG laser ($\lambda = 266$ nm). We also discuss the optimisation of YIG growth in the multi-PLD chamber.

3.1.1. Ablation of YIG with the KrF laser

First of all, a deposition test (sample E1) was performed under the same conditions as Y20, the best YIG film grown on YAG in our single-beam single-target ("single-PLD") system [9], except for substrate temperature ($T \approx 1150$ K), which is limited by the heating method in our multi-PLD system: KrF laser fluence was set at $F_{KrF} \approx 3$ J/cm^2, pulse repetition rate at $f_{KrF} \approx 20$ Hz, oxygen pressure at $P_{O2} \approx 1$ Pa and target–substrate distance d at ≈ 6 cm. As shown in Table 2, there are only two big differences between Y20 and E1: film thickness and the FMR linewidth (ΔH). The lower film thickness in E1, compared to Y20, is due to the continuous tilting of the targets during their ablation and to the target configuration in the multi-PLD chamber, where the three target holders are symmetrically off-axis with respect to the substrate, thus causing a lower deposition rate, compared to film growth in the single-PLD system with the on-axis configuration. The FMR linewidth is almost twice the value of Y20, most likely because of the lower substrate temperature: in fact, the FMR linewidth of E1 is roughly the same as that of Y11 ($\Delta H \approx 2.9$ mT), grown under similar conditions ($T \approx 1150$ K, $d =$ 6 cm, $P_{O2} \approx 3.3$ Pa) [9].

Table 2
Deposition conditions and results of samples E1–E4. Sample Y20 is shown as a reference. "Conc." stands for concentration.

ID	P_{O_2} [Pa]	Target–substrate distance d [cm]	Thickness t [μm]	Y conc. [formula number]	Fe conc. [formula number]	Fe/Y	ΔH [mT]	Sample colour
Y20	1	6	2.4	3.55	4.45	1.25	1.8	Yellow
E1	1	6	1.4	3.54	4.46	1.26	3.0	Yellow
E2	1	4	3.3	3.36	4.64	1.38	7.2	Dark yellow
E3	3.4	4	2.5	3.52	4.48	1.27	3.9	Yellow
E4	6.8	4	2	3.47	4.53	1.31	6.6	Yellow